Overexpression of cdk4 and cyclinD1 triggers greater expansion of neural stem cells in the adult mouse brain

Benedetta Artegiani,[1] Dirk Lindemann,[1,2] and Federico Calegari[1]

[1]German Research Foundation Research Center and Cluster of Excellence for Regenerative Therapies and [2]Institute of Virology, Medical Faculty, Dresden University of Technology, 01307 Dresden, Germany

Neural stem cells (NSCs) in the adult mammalian brain generate neurons and glia throughout life. However, the physiological role of adult neurogenesis and the use of NSCs for therapy are highly controversial. One factor hampering the study and manipulation of neurogenesis is that NSCs, like most adult somatic stem cells, are difficult to expand and their switch to differentiation is hard to control. In this study, we show that acute overexpression of the cdk4 (cyclin-dependent kinase 4)–cyclinD1 complex in the adult mouse hippocampus cell-autonomously increases the expansion of neural stem and progenitor cells while inhibiting neurogenesis. Importantly, we developed a system that allows the temporal control of cdk4–cyclinD1 overexpression, which can be used to increase the number of neurons generated from the pool of manipulated precursor cells. Beside providing a proof of principle that expansion versus differentiation of somatic stem cells can be controlled in vivo, our study describes, to the best of our knowledge, the first acute and inducible temporal control of neurogenesis in the mammalian brain, which may be critical for identifying the role of adult neurogenesis, using NSCs for therapy, and, perhaps, extending our findings to other adult somatic stem cells.

CORRESPONDENCE
Federico Calegari:
federico.calegari@crt-dresden.de

Abbreviations used: DCX, doublecortin; GFAP, glial fibrillary acidic protein; MLV, murine leukemia virus; NSC, neural stem cell.

After embryonic development, neural stem cells (NSCs) remain in specific regions of the adult mammalian brain where they become a source of new neurons and glia throughout life (Zhao et al., 2008; Kriegstein and Alvarez-Buylla, 2009). Currently, great efforts are invested in understanding the physiological role of adult neurogenesis and manipulating this process for therapy. Apart from tissue homeostasis (Imayoshi et al., 2008), adult neurogenesis is considered to be involved in superior brain functions such as learning and memory (Kempermann, 2008; Deng et al., 2010), and controlling this process is believed to be important for developing novel therapies for neurodegenerative diseases or injuries of the central nervous system (Goldman, 2005; Lindvall and Kokaia, 2006).

However, a major factor limiting the study and use of adult NSCs is that, like for many other somatic stem cells, controlling their expansion versus differentiation in vivo has proven to be extremely difficult. In fact, in contrast to embryonic development, the vast majority of adult NSCs in vivo are quiescent (Kempermann et al., 2004; Zhao et al., 2008; Kriegstein and Alvarez-Buylla, 2009; Lugert et al., 2010). Moreover, the few NSCs that divide do so to self-renew and generate more differentiated progenitors, giving rise to terminally committed neuroblasts that are soon consumed to generate postmitotic neurons (Kempermann et al., 2004; Zhao et al., 2008; Kriegstein and Alvarez-Buylla, 2009). In essence, NSCs in the adult brain are found in limited numbers, and no methodology has been developed to promote their expansion to ultimately increase neurogenesis in vivo.

In studying mouse embryonic development, our laboratory has recently found that an acute overexpression of positive regulators of cell cycle progression, in particular the cdk4 (cyclin-dependent kinase 4)–cyclinD1 complex (referred to for simplicity as 4D), can be used to expand neural stem and progenitor cells while

B. Artegiani and F. Calegari's present address is Max Planck Institute of Molecular Cell Biology and Genetics, 01307 Dresden, Germany.

The Rockefeller University Press $30.00
J. Exp. Med. Vol. 208 No. 5 937-948
www.jem.org/cgi/doi/10.1084/jem.20102167

The Journal of Experimental Medicine

inhibiting their switch to neurogenesis (Lange et al., 2009). Essentially, this and other studies (Salomoni and Calegari, 2010) indicated that shortening the cell cycle of neural stem and progenitor cells during embryonic brain development alone is sufficient to inhibit their differentiation and increase their proliferative potential.

Although important for a better understanding of brain development, these findings may initially appear irrelevant to the field of adult neurogenesis and, in particular, for the potential use of NSCs in therapy. Moreover, findings in developing embryos seem to be at direct odds with observations in the adult mouse brain, where stem cells with higher proliferative potential have been shown to have longer instead of shorter (Calegari et al., 2005; Arai et al., 2011) cell cycles than more committed progenitors types (Cameron and McKay, 2001; Hayes and Nowakowski, 2002; Seri et al., 2004). Finally, another major difference between embryonic and adult NSCs is that the latter are mostly quiescent (Lugert et al., 2010), thus making it difficult, if not impossible, to extrapolate findings about the role of cell cycle length from the developing to the adult brain.

For these reasons, in this study, we decided to directly investigate the effects of 4D overexpression on proliferation versus differentiation of neural stem and progenitor cells in the adult mouse brain. To this end, the abundance of cells immunoreactive for different markers of neural precursors were analyzed at different times after stereotaxic infection with multicistronic viral particles triggering the expression of cdk4, cyclinD1, and GFP as a fluorescent reporter. More importantly, we sought to develop a system that would allow the conditional on/off control of 4D overexpression when desired. We thought that this would be important toward manipulating the fate of neural stem and progenitor cells in vivo, i.e., their propensity to divide to generate additional stem and progenitor cells (expansion) or to generate neurons (differentiation), which may have a great impact in the field of stem cell research and their use in medicine.

RESULTS

Coexpression of a catalytically active 4D complex and GFP by lentiviruses

To overexpress the 4D complex together with a reporter protein that would allow targeted cells to be identified, we generated HIV-1–based lentiviruses encoding for (a) cdk4, (b) cyclinD1, and (c) GFP with a nuclear localization signal to reliably count individual infected cells (together referred to as 4DG viruses; Fig. 1 a, bottom). The three transgenes were linked by sequences encoding for 2A peptides (de Felipe et al., 2006), which allows the stoichiometric expression of multiple genes after viral infection in the adult brain (Tang et al., 2009).

Coexpression of GFP and catalytic activity of the ectopic 4D complex after infection with 4DG as compared with GFP control (Fig. 1 a, top) viruses were validated by immunocytochemistry and

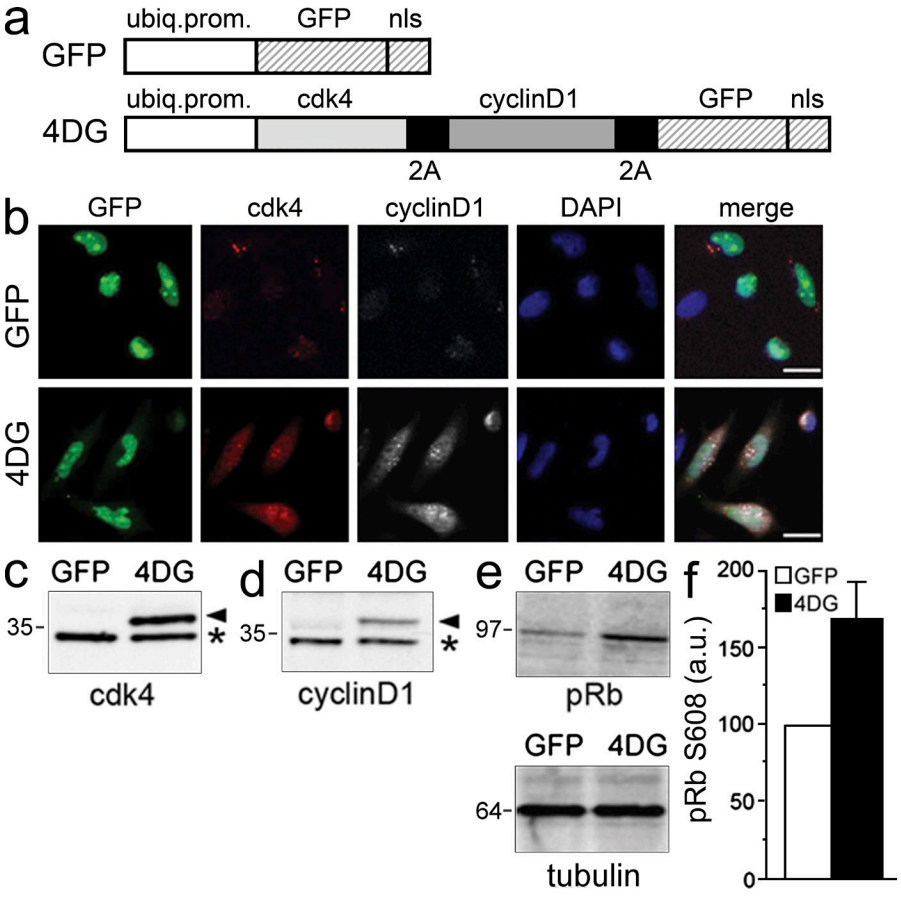

Figure 1. Coexpression of catalytically active 4D complex and GFP by lentiviruses. (a) Control GFP (top) and 4DG (bottom) viral transfer vectors used in this study. Note the use of the ubiquitin promoter (ubiq. prom.), the presence of the nuclear localization signal (nls) in both vectors, and the use of 2A sequences to link the three transgenes in 4DG. (b) Fluorescence pictures of HeLa cells after GFP (top) or 4DG (bottom) infection and immunocytochemistry for cdk4 (red), cyclinD1 (white), and DAPI counterstaining (blue) representative of two independent experiments. Bars, 20 µm. (c and d) Western blot analyses of GFP- or 4DG-infected HeLa cells using cdk4 (c) or cyclinD1 (d) antibodies. Note the higher molecular mass (kilodaltons) of ectopic (arrowheads), relative to endogenous (asterisks), cdk4 and cyclinD1 proteins in samples infected with 4DG viruses caused by fusion of the cell cycle regulators with a 2A peptide. (e and f) Western blot analyses (e) and quantification (f) of retinoblastoma (pRb) using antibodies specific for phosphorylated Ser608 (e, top) upon tubulin normalization as loading control (e, bottom); values in controls are defined as GFP = 100 arbitrary units (a.u.); $n = 2$; error bar represents SEM.

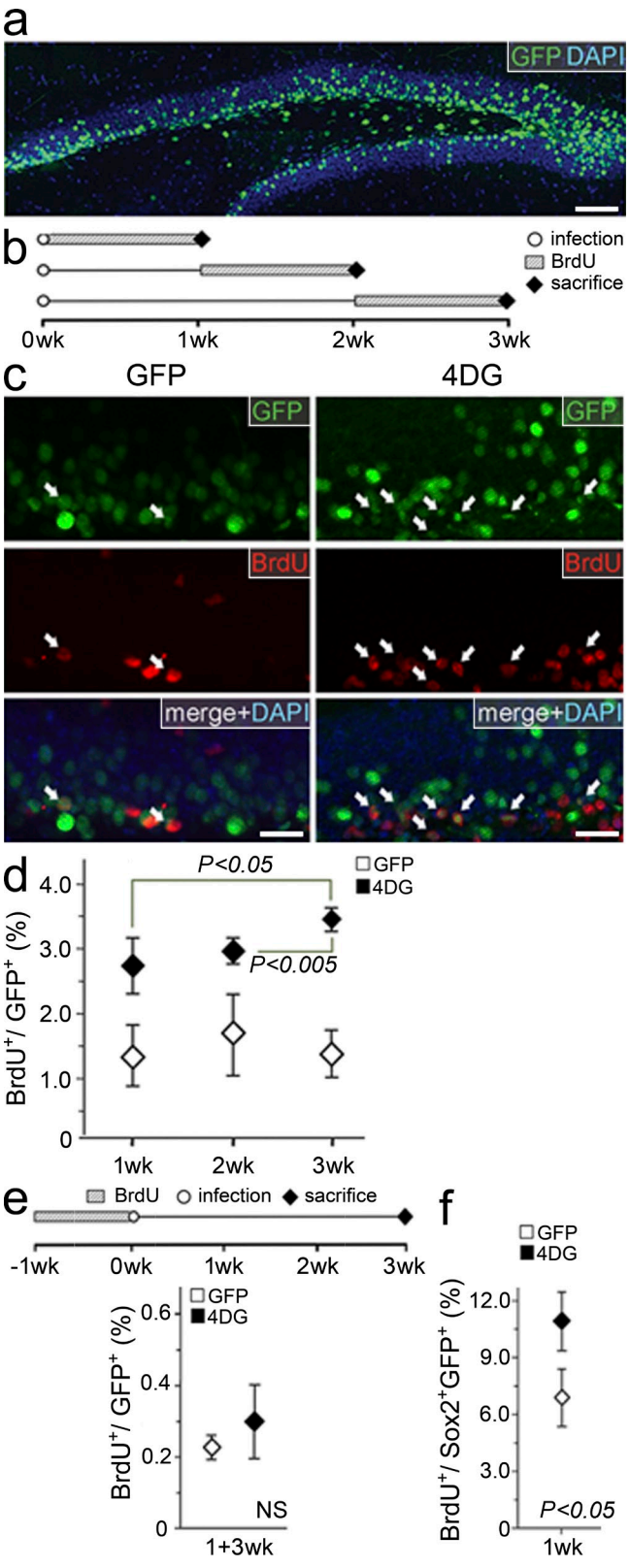

Figure 2. 4DG increases the proliferation in the adult hippocampus. (a) Composite picture of a 40-µm thick vibratome section through the mouse hippocampus showing GFP fluorescence and DAPI counterstaining 3 wk after infection with GFP viruses. (b) Layout of the experiments performed to investigate effects on proliferation. BrdU administration and sacrifice are indicated at 1, 2, or 3 wk after infection (0 wk). (c) Fluorescence pictures of the granular and subgranular zone 3 wk after infection with GFP (left) or 4DG (right) viruses and 7 d of BrdU administration as depicted in b, followed by immunohistochemistry for GFP (top), BrdU (middle), and DAPI counterstaining (shown as merge; bottom). Arrows indicate $BrdU^+$ GFP^+ cells. (d) Quantification of the proportion (percentage) of $BrdU^+$ cells as in c after GFP or 4DG infection ($P < 0.05$ between any GFP and 4DG time point; significance among 4DG time points are indicated). (e) Layout of the experiments (top) and quantifications (bottom) to determine the proportion of label (BrdU)-retaining cells after GFP or 4DG infection. (f) Proportion (percentage) of $BrdU^+$ cells within the population of $Sox2^+$ GFP^+ 1 wk after GFP or 4DG infection and 1 wk of BrdU exposure as shown in b (top). (d–f) Data are the mean of three (six in d, 1 wk; four in f, GFP) hippocampi of different animals; error bars represent SD; differences between GFP time points in d and between GFP and 4DG in e are not significant. Bars: (a) 100 µm; (c) 20 µm.

Western blot analyses on HeLa cells (Fig. 1, b–f). We found that 3 d after infection, ∼70–80% of cells displayed nuclear GFP fluorescence with only a subpopulation of control, GFP-infected cells being immunoreactive for cdk4 and/or cyclinD1, whereas the vast majority of cells infected with 4DG viruses were positive for both. In addition, the immunoreactivity levels of the two cell cycle regulators in control conditions were overall lower than those observed after infection with 4DG (Fig. 1 b).

Western blot analyses using antibodies against cdk4 or cyclinD1 showed an efficient cleavage of the 2A peptides and an overall doubling in the total levels of cdk4 and cyclinD1 proteins (Fig. 1, c and d, respectively). Functionality of the overexpressed cell cycle regulators was investigated using phosphorylation-specific antibodies to quantify the levels of retinoblastoma phosphorylated at Ser608, a direct target of the 4D complex (Zarkowska and Mittnacht, 1997). This revealed a 60% increase in 4DG-infected cells relative to control (Fig. 1, e and f). Thus, infection with 4DG viruses can be used to trigger the overexpression of a catalytically active 4D complex.

4D overexpression increases the proliferation of neural stem and progenitor cells in the adult hippocampus

For in vivo analyses, control GFP or 4DG viruses were stereotaxically injected in the hippocampus of 6–10-wk-old mice. We decided to investigate the effect of 4D overexpression in the hippocampus and not in the lateral ventricle, the second neurogenic niche of the mouse brain, because of the presence of ependymal cells in the latter region (Kriegstein and Alvarez-Buylla, 2009), which may confuse our analysis. Mice were sacrificed 1–3 wk after infection, and brains were stereologically analyzed to measure the induced effects in the subpopulation of GFP^+ cells.

In general, infection efficiency was high with both GFP and 4DG viruses, leading to ∼10,000–30,000 GFP^+ cells throughout the dentate gyrus of the whole hippocampus (Fig. 2 a and Fig. S2). The effects on proliferation were investigated by calculating the proportion of $BrdU^+$ cells within the population of GFP^+ cells 1, 2, or 3 wk after viral infection,

with BrdU being administered during the 7 d preceding sacrifice (Fig. 2, b–d).

As expected, the proportion of $BrdU^+$ cells was modest in control conditions (1.56 ± 0.18% when the three time points were averaged; Fig. 2 d, open diamonds), as most cells in the dentate gyrus do not divide. In contrast, after 4DG infection, the proportion of $BrdU^+$ cells increased by between 1.7- and 2.2-fold (2.69 ± 0.51%, 2.97 ± 0.15%, and 3.47 ± 0.15% at 1, 2, or 3 wk, respectively; Fig. 2 d, closed diamonds). Interestingly, although in controls the proportion of $BrdU^+$ cells remained constant, the increase observed after 4DG infection became more prominent at increasing survival times (~20% and 30% increase at 3 wk relative to 2 wk and 1 wk, respectively; Fig. 2 d; closed diamonds), suggesting an expansion of the population of cycling cells over time.

This increase in $BrdU^+$ cells after 4DG infection could be attributed to at least four different effects such as (1) quiescent NSCs entering the cell cycle, (2) a faster proliferation rate of cycling cells, (3) increased proliferative divisions at the expense of neurogenic divisions, and/or (4) lethality of postmitotic neurons, which would increase the relative proportion of dividing cells but not their absolute numbers.

To investigate the first possibility, we assessed the proportion of label-retaining cells after GFP or 4DG infection. BrdU was administered for 7 d before viral infection, and brains were analyzed 3 wk later (Fig. 2 e, top). No significant change was found in the proportion of $BrdU^+$ cells within the population of GFP^+ cells in the subgranular zone (0.22 ± 0.04% and 0.30 ± 0.11% for GFP and 4DG infection, respectively; Fig. 2 e, bottom), indicating that 4D overexpression is not sufficient to induce cell cycle reentry of quiescent NSCs.

We then investigated the possibility that 4D overexpression may increase the proliferation rate of cycling precursors by assessing BrdU incorporation within the population of cells positive for Sox2, a marker expressed in both type 1 and type 2 cells (Suh et al., 2007; Hodge et al., 2008; Lugert et al., 2010). We found that as early as at 1 wk after infection, the proportion of $BrdU^+$ cells within the subpopulation of $Sox2^+$ GFP^+ cells was significantly higher in 4DG-infected brains (7.28 ± 1.49% and 10.63 ± 1.61% for GFP and 4DG, respectively; Fig. 2 f). Altogether, these data suggest that acute overexpression of the 4D complex in the adult mouse hippocampus increases the proportion of cycling cells and their proliferative rate without inducing cell cycle reentry of quiescent NSCs.

4D overexpression increases the expansion of neural stem and progenitor cells at the expense of neurogenesis

To investigate another possible reason for the higher proportion of $BrdU^+$ cells upon 4D overexpression (Fig. 2 d), i.e., whether 4DG infection increased the number of proliferative divisions at the expense of neurogenic divisions, we quantified the abundance of NSCs, progenitor cells, neuroblasts, and neurons within the population of GFP^+ cells 3 wk after infection with GFP or 4DG viruses. We identified type 1 NSCs as cells positive for (a) glial fibrillary acidic protein (GFAP; but negative for the astrocyte marker S100-β), (b) nestin, or (c) Sox2 (but negative for the type 2 marker Tbr2; Kempermann et al., 2004; Hevner et al., 2006; Suh et al., 2007; Hodge et al., 2008). Using these three independent criteria, we found that the proportion of type 1 cells overall doubled in 4DG-infected brains relative to GFP controls ($GFAP^+$ $S100\text{-}\beta^-$ from 2.51 ± 0.17% to 5.29 ± 0.71%; $nestin^+$ from 2.21 ± 0.22% to 5.65 ± 0.93%; $Sox2^+$ $Tbr2^-$ from 2.01 ± 0.37% to 3.54 ± 0.28% in GFP- and 4DG-infected brains, respectively; Fig. 3, a–c and e). Moreover, the proportion of $Tbr2^+$ cells was also increased by a similar magnitude (from 0.61 ± 0.18% to 1.46 ± 0.38% for GFP and 4DG, respectively; Fig. 3, c and e), indicating a similar effect of 4D overexpression on type 2 progenitor cells.

Finally, doublecortin (DCX) was used to assess the abundance of type 3 neuroblasts and newborn neurons (Kempermann et al., 2004; Hevner et al., 2006; Zhao et al., 2008). Three histological and morphological criteria were used to discriminate between the two cell types. Specifically, DCX^+ type 3 neuroblasts were confined to the subgranular zone and had a polygonal shape and nuclei oriented parallel to the subgranular zone (Figs. 3 d and 4 b and Fig. S1). In contrast, DCX^+ newborn neurons were mainly located in the granular zone and had an elongated shape with long processes and nuclei perpendicular to the subgranular zone (Figs. 3 d and 4 b and Fig. S1). This approach was validated by double staining for DCX and NeuN, a marker of mature neurons (Kempermann et al., 2004; Zhao et al., 2008), showing that the majority of DCX^+ cells scored as neurons were $NeuN^+$, whereas essentially all DCX^+ cells scored as type 3 neuroblasts were $NeuN^-$ (Fig. S1).

With regard to the effect of 4D, we found no significant difference on DCX^+ type 3 neuroblasts (0.94 ± 0.03% vs. 1.27 ± 0.47% for GFP and 4DG, respectively), whereas a major reduction in DCX^+ newborn neurons was observed (1.57 ± 0.09% vs. 0.63 ± 0.20% for GFP and 4DG, respectively; Fig. 3, d and e). In addition, in control brains, it was found that within the population of DCX^+ cells, the minority were type 3 neuroblasts (37 ± 2%) while the majority were newborn neurons (63 ± 2%; Fig. 3 f, top), whereas these proportions were the reverse in 4DG-infected brains with the majority of DCX^+ cells being type 3 neuroblasts (66 ± 12%) and a minority being neurons (34 ± 12%; Fig. 3 f, bottom). Altogether, these data are consistent with a cell fate change of neural stem and progenitor cells upon 4D overexpression and, in particular, with an increase in the proportion of proliferative divisions at the expense of neurogenic divisions.

4D overexpression in newborn neurons does not affect their survival or maturation

It was particularly important for our study to investigate the possibility that 4D overexpression in newborn neurons might have unspecific effects such as to affect their survival and/or maturation. In fact, the increase in the relative proportion of proliferating stem and progenitor cells described in the previous section may simply be explained, at least in part, by an increased lethality of newborn neurons.

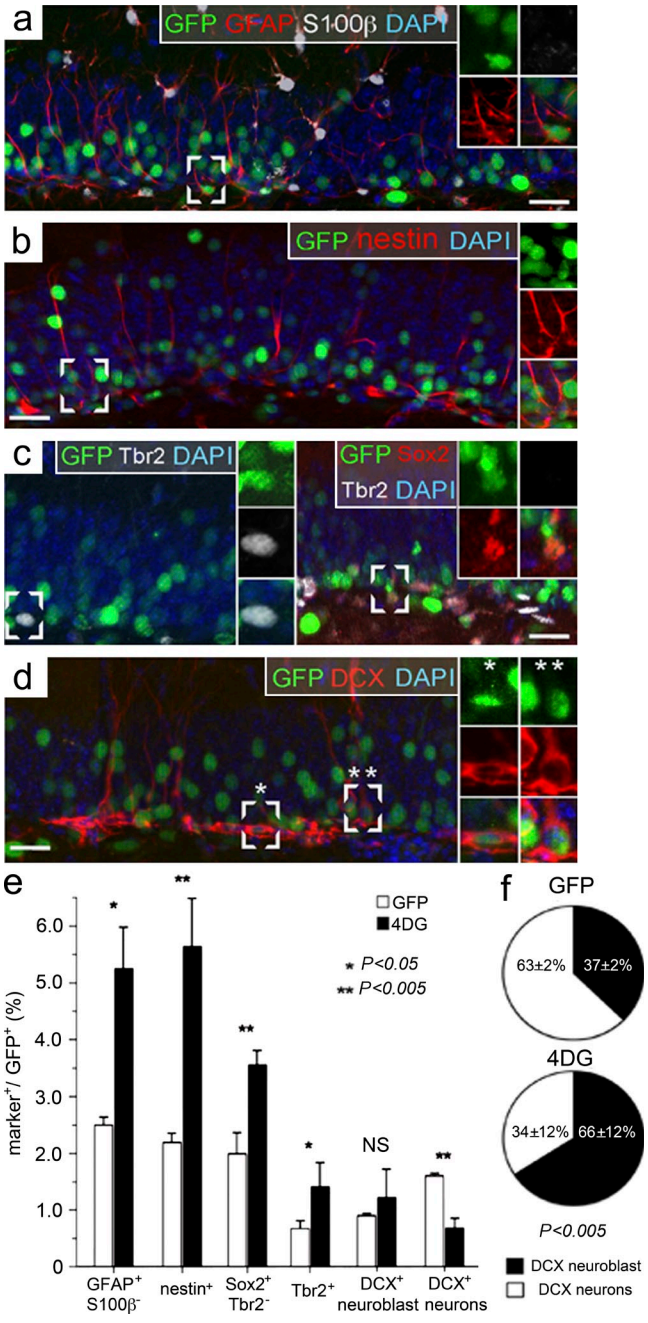

Figure 3. 4DG increases the expansion of stem and progenitor cells at the expense of neurogenesis. (a–d) Fluorescence pictures of the granular and subgranular zone 3 wk after infection with GFP viruses and immunohistochemistry for GFP in combination with various cellular markers and DAPI counterstaining. White frames outline GFP$^+$ cells scored as GFAP$^+$ S100-β$^-$ (a), nestin$^+$ (b), Tbr2$^+$ (c, left), Sox2$^+$ Tbr2$^-$ (c, right), DCX$^+$ neuroblast (d, one asterisk, left), and DCX$^+$ neuron (d, two asterisks, right) cells, whose individual channels are shown magnified in the right insets. Bars, 20 µm. (e) Proportions (percentages) of the different GFP$^+$ cell types as shown in a–d 3 wk after GFP or 4DG infection (all GFP$^+$ cells = 100%). (f) Pie graphs showing the proportion (percentage) of DCX$^+$ type 3 neuroblasts and DCX$^+$ neurons 3 wk after GFP (top) or 4DG (bottom) infection (all DCX$^+$ cells = 100%). (e and f) Data are the mean of at least three hippocampi of different animals; error bars represent SD; p-values are indicated.

Because of the long temporal gaps between infection and analysis in our experiments, we thought that apoptotic assays would not be the appropriate technique with which to examine the possibility of increased death of newborn neurons. Therefore, to assess neuronal death, we sought to overexpress 4D preferentially in type 3 neuroblasts and newborn neurons but to a lesser extent in type 1 NSCs and type 2 progenitors, in which the 4D effect was more prominent. For this, we took advantage of the fact that (a) a significantly higher fraction of type 2 progenitors and type 3 neuroblasts, as compared with NSCs, undergo mitosis at any given time (Cameron and McKay, 2001; Hayes and Nowakowski, 2002; Seri et al., 2004) and (b) the onset of transgene expression after viral infection of a mitotic mother cell will occur in her daughters (Fig. 4 a). Thus, we cloned the 4D cassette in a transfer vector of murine leukemia virus (MLV; van Praag et al., 2002), which in contrast to HIV-1 transduces its genome only in mitotic cells.

Moreover, because compared with HIV-1 infection identification of individual cells was expected to be easier as a result of the scarcity of mitotic cells and cytoplasmic fluorescence is superior to nuclear fluorescence to assess neuronal identity, we decided to use MLV with a cytoplasmic RFP reporter (4DR) that was validated as already described for 4DG viruses (unpublished data). Thus, RFP or 4DR viruses were injected in the hippocampus, and the proportion of DCX$^+$ type 3 neuroblasts and DCX$^+$ newborn neurons were assessed in RFP$^+$ cells 3 wk later (Fig. 4 b).

We found that the vast majority of RFP$^+$ cells after infection with RFP or 4DR were DCX$^+$, with this proportion being essentially the same in the two conditions (89 ± 3% and 94 ± 2%, respectively; Fig. 4 c). Within the population of RFP$^+$ DCX$^+$ cells, there was also no change detected in the abundance of type 3 neuroblasts as compared with newborn neurons (25 ± 1% and 75 ± 2% vs. 24 ± 8% and 76 ± 8%, respectively, in RFP- or 4DR-infected brains; Fig. 4 d). In addition, the overall morphology of the RFP$^+$ DCX$^+$ newborn neurons and the location of their soma within the granular zone were undistinguishable between the two conditions (unpublished data).

Altogether, these data indicate that 4D overexpression does not have any major effect neither on the fate of type 3 neuroblasts nor on the survival, maturation, or migration of DCX$^+$ newborn neurons. Thus, together with our previous results (Fig. 3), this strongly suggests that the major effect of 4D overexpression is to change the fate of cycling type 1 NSCs and type 2 progenitors.

A transitory 4D overexpression increases neuronal production from the manipulated pool of NSCs

If 4D overexpression should truly increase the expansion of NSCs, it would be reasonable to expect that a transitory rather than continuous overexpression of 4D should induce a phase of expansion followed by a phase of physiological neurogenesis. Therefore, as a result of the increased expansion in the first phase, a greater production of neurons should ensue in the second phase.

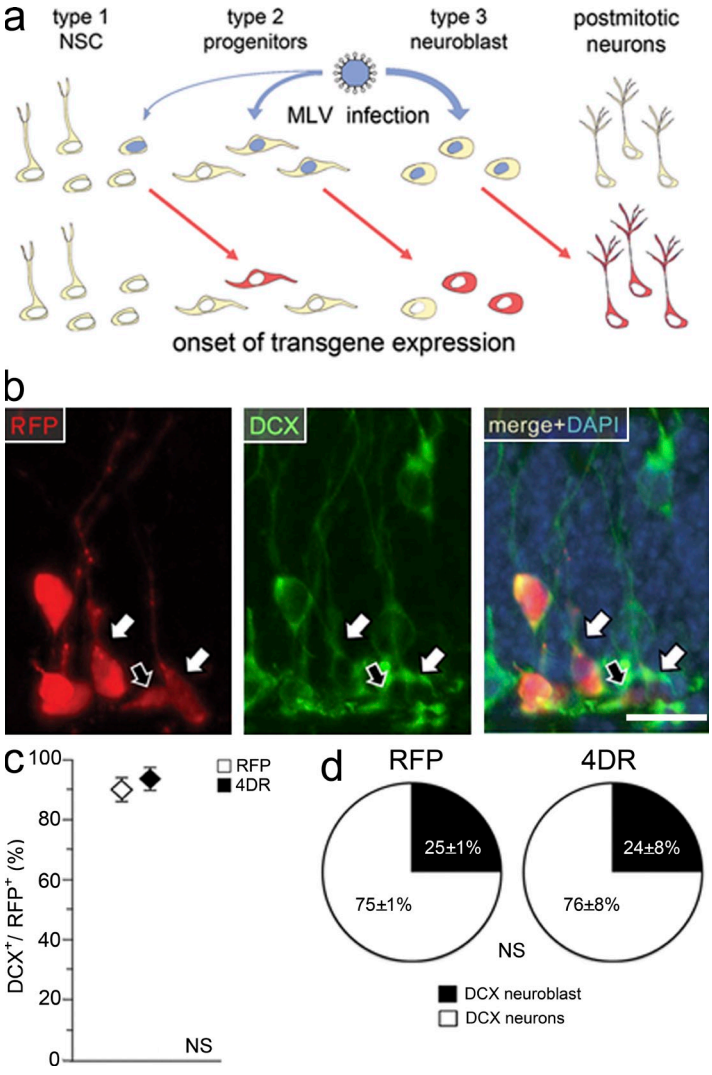

Figure 4. 4D overexpression does not affect survival of newborn neurons. (a) Schematic representation of the effect induced by MLV infection with efficiency of infection (top; blue arrows) being proportional to the proliferation rate of stem or progenitor cells (from left to right, respectively). Onset of transgene expression (bottom) would preferentially occur in the daughters (red arrows and cells) of infected mother cells (top; blue nuclei) with the majority of red cells being DCX$^+$ type 3 neuroblast or newborn neurons. (b) Fluorescence pictures of the granular and subgranular zone 3 wk after RFP infection and immunohistochemistry for RFP (left), DCX (middle), and DAPI counterstaining (shown as merge; right). Arrows indicate cells scored as DCX$^+$ neuroblasts (black) or DCX$^+$ neurons (white). Bar, 20 µm. (c) Proportion (percentage) of DCX$^+$ cells within the population of RFP$^+$ cells 3 wk after RFP or 4DR infection. (d) Pie graphs showing the proportion (percentage) of DCX$^+$ neuroblasts and DCX$^+$ neurons 3 wk after RFP (left) or 4DR (right) infection (all DCX$^+$ cells = 100%). (c and d) Data are the mean of three hippocampi of different animals; error bars represent SD; differences are not significant.

To investigate this possibility, we sought to infect nestin-CreER^{t2} mice (Imayoshi et al., 2008) and to use loxP sites to remove the 4D cassette upon tamoxifen administration. Because in this system only a small proportion of cells are expected to undergo recombination as the result of expression of CreER^{t2} only in nestin$^+$ NSCs, we needed a system that would allow us to identify those cells in which recombination had occurred. Thus, we changed the position of the transgenes to have the 4D cassette downstream instead of upstream of GFP and placed loxP sites to remove its nuclear localization signal together with the cell cycle regulators (construct referred to as G^{lox}4D; Fig. 5 a, bottom). This strategy would allow cells that underwent recombination and their progeny to be identified by the redistribution of GFP from the nucleus to the cytoplasm. For control experiments, GFP viruses were generated in which loxP sites were used to remove only the nuclear localization signal (GFP^{lox}; Fig. 5 a, top). GFP^{lox} or G^{lox}4D viruses were injected in the hippocampus of nestin-CreER^{t2} mice, and 3 wk later, mice were exposed to tamoxifen for 2 d and then left for an additional 2 wk before sacrifice (Fig. 5 b).

First, we found that the proportion of cells with cytoplasmic (GFP^{cyt}) as compared with nuclear (GFP^{nuc}) GFP was 2.9-fold higher in brains infected with G^{lox}4D as compared with GFP^{lox} viruses (2.36 ± 0.75% and 6.86 ± 1.61% for GFP^{lox} and G^{lox}4D, respectively; Fig. 5, c and d) and that essentially no GFP^{cyt+} cell could be observed neither in GFP^{lox}- nor G^{lox}4D-infected brains upon administration of vehicle alone (not depicted). Clearly, the higher proportion of GFP^{cyt+} cells upon G^{lox}4D infection was expected because of the very similar effect of 4D on the expansion of nestin$^+$ type 1 cells (Fig. 3 e), which would increase the proportion of CreER^{t2}-expressing cells undergoing recombination and becoming GFP^{cyt+} upon tamoxifen administration.

Second, to investigate whether upon excision of the 4D cassette stem and progenitor cells could resume a physiological balance between proliferation and neurogenesis, we restricted our analysis to the subpopulation of GFP^{cyt+} cells, i.e., those generated in the 2 wk after tamoxifen administration by nestin$^+$ cells that underwent recombination and thus did not express the ectopic 4D complex any longer. Within this population, we found that the proportion of DCX$^+$ type 3 neuroblasts as compared with newborn neurons was very similar in GFP^{lox} (76 ± 11% neurons)- and G^{lox}4D (83 ± 3% neurons)-infected brains (Fig. 5 e), implying that removal of the 4D cassette allows stem and progenitor cells to resume physiological neurogenesis.

Finally, third, to investigate whether our approach ultimately allows a greater generation of neurons from the pool of 4D-overexpressing cells as compared with controls, we assessed the proportion of all DCX$^+$ newborn neurons relative to all GFP$^+$ cells, irrespective of whether GFP^{cyt+} or GFP^{nuc+}, and found an increase by 1.9-fold in G^{lox}4D- as compared with GFP^{lox}-infected brains (2.22 ± 0.72% and 4.19 ± 0.57% for GFP^{lox} and G^{lox}4D, respectively; Fig. 5, c and f), which is even more remarkable if one considers that at 3 wk the proportion of DCX$^+$ neurons in 4DG-infected brains was less

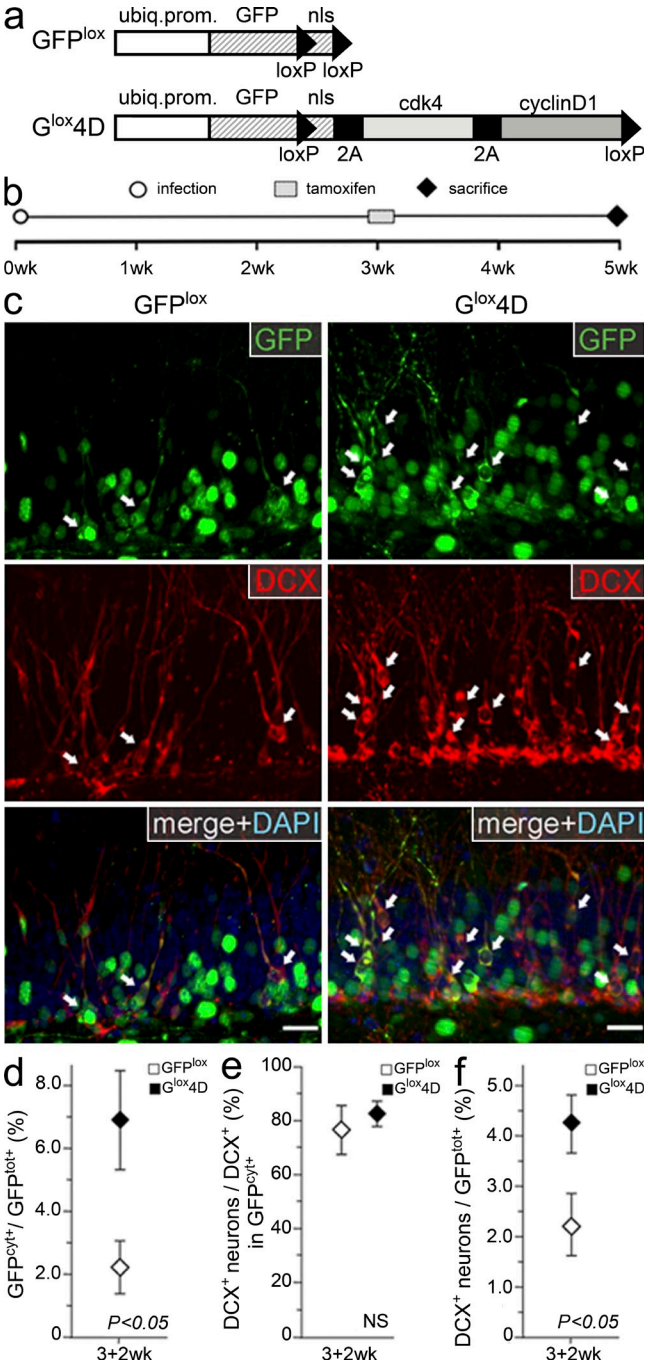

Figure 5. A transient 4D overexpression increases the generation of neurons. (a) GFP^{lox} (top) and G^{lox}4D (bottom) transfer vectors used for the temporal control of 4D overexpression. Note the presence of loxP sites to remove the nuclear localization signal (nls) alone (GFP^{lox}) or together with the 4D cassette (G^{lox}4D). (b) Layout of the experiments with a 2-d administration of tamoxifen and sacrifice occurring at 3 wk and 5 wk after viral infection, respectively, in nestin-CreER^{t2} mice. (c) Fluorescence pictures of the granular and subgranular zone 3 wk after infection with GFP^{lox} (left) or G^{lox}4D (right) viruses and immunohistochemistry for GFP (top), DCX (middle), and DAPI counterstaining (shown as merge; bottom). DCX$^+$ GFP^{cyt+} cells are indicated by arrows. Bars, 20 µm. (d–f) Proportion (percentage) of GFP^{cyt+} cells within the GFP$^+$ population (d), DCX$^+$ neurons within the DCX$^+$ GFP^{cyt+} population (e), and DCX$^+$ neurons within all GFP$^+$ cells (f) after GFP^{lox} or G^{lox}4D infection as depicted in b. Data are the mean of at least three hippocampi of different animals; error bars represent SD; p-values are indicated; difference in e is not significant. No significant difference was found between quantifications shown in panel e, Fig. 4 d, and controls in Fig. 3 f (top; analysis of variance $F > 0.55$).

than half that observed in the control (Fig. 3 e). In essence, stopping 4D overexpression not only allowed the recovery of the deficit of neurons that had occurred in the previous weeks but also led to their overproduction, which further corroborates the conclusion that 4D overexpression induces the expansion of neural precursors rather than the lethality of newborn neurons.

The effects of 4D are cell intrinsic

Several factors are known to be released within the neurogenic niche to regulate the proliferation of NSCs as exemplified by the release of Wnt by astrocytes (Lie et al., 2005) and the intimate relationship between NSCs and the vasculature (Shen et al., 2008; Tavazoie et al., 2008). Considering that the HIV-1 viruses used in our experiments target all cell types within the niche, it is in principle possible that the phenotype observed in neural stem and progenitor cells might be caused by cell extrinsic effects induced by 4D overexpression in other cells.

To investigate the possible effects of 4D on the expansion of other cell types, we quantified the proportion of S100-β$^+$ astrocytes, Olig2$^+$ oligodendrocytes, and VEGF-R$^+$ (vascular endothelium growth factor receptor) endothelial cells among GFP$^+$ cells 3 wk after infection with GFP or 4DG viruses. No significant difference was observed in the proportion of glial cells (S100-β$^+$, 4.82 ± 0.69% vs. 5.37 ± 1.07; and Olig2$^+$, 1.60 ± 0.39% vs. 1.23 ± 0.38% for GFP and 4DG, respectively; Fig. 6, a–c), whereas essentially no VEGF-R$^+$ cell could be found among the GFP$^+$ population in either condition (not depicted).

Moreover, cell extrinsic effects of 4D overexpression within the niche were investigated by assessing proliferation among noninfected cells. We reasoned that a manipulation of the niche should be equally effective on stem and progenitor cells irrespective of whether GFP$^+$ or GFP$^-$. Thus, BrdU$^+$ GFP$^-$ cells were counted 3 wk after infection with GFP or 4DG viruses, with BrdU being administered during the 7 d preceding sacrifice. Values were normalized per volume of granular plus subgranular zone, which held essentially identical values in either condition (13.2 ± 3.5 × 10^3 cells/mm^3 vs. 12.8 ± 1.1 × 10^3 cells/mm^3 for GFP and 4DG, respectively; Fig. 6 d).

Finally, to investigate whether 4D overexpression specifically influenced the fate of type 1 NSCs in a cell-autonomous manner, we decided to induce 4D overexpression in all cell subpopulations within the niche except for nestin$^+$ cells. To achieve this, we infected nestin-CreER^{t2} mice with G^{lox}4D viruses, but this time we administered tamoxifen after only 24 h to prevent the expression of the 4D complex specifically in nestin$^+$

cells (Fig. 6 e). Similar to our previous experiments (Fig. 2 b), brains were collected 3 wk later, with BrdU being administered during the 7 d preceding sacrifice. Under these conditions, the proportion of $BrdU^+$ cells in the GFP^+ population of $G^{lox}4D$-infected brain was essentially identical to what has been observed 3 wk after infection with GFP control viruses (1.46 ± 0.21% vs. 1.63 ± 0.3% for GFP and $G^{lox}4D$, respectively) and significantly lower than 4DG infection (3.47 ± 0.15%; Figs. 2 d and 6 e [bottom]). Altogether, these data indicate that 4D overexpression within the hippocampus specifically and cell-autonomously influences the fate of NSCs with minimal, if any, effect on other cell types.

DISCUSSION

4D regulates the expansion of neural stem and progenitor cells

In this study, we found that 4D expression can be used to manipulate the balance between proliferative and neurogenic divisions of adult neural stem and progenitor cells. This manipulation was found to be reversible whereby a transitory phase of expansion, followed by a physiological switch to neurogenesis, ultimately allowed us to double the number of neurons generated by the pool of manipulated NSCs.

These data corroborate previous findings in the embryonic mouse cortex, extending the cell cycle length hypothesis to adult somatic stem cells (Salomoni and Calegari, 2010). Importantly, finding a similar effect of 4D overexpression in stem cells of the developing embryo and the adult brain was rather surprising considering that, contrary to embryonic development, adult NSCs with higher proliferative potential have longer instead of shorter cell cycles than more committed progenitors (Cameron and McKay, 2001; Hayes and Nowakowski, 2002; Seri et al., 2004; Calegari et al., 2005; Arai et al., 2011). Moreover, in the developing cortex, the major effect of 4D overexpression was to increase the expansion of more committed progenitor types (i.e., basal progenitors) with essentially no effect on NSCs (i.e., apical progenitors; Lange et al., 2009). In contrast, in the adult brain, we observed a similar increase in the proportion of both type 1 NSCs and type 2 progenitors but essentially no effect on more committed type 3 neuroblasts that may be considered the cell biological equivalent of the embryonic basal progenitors.

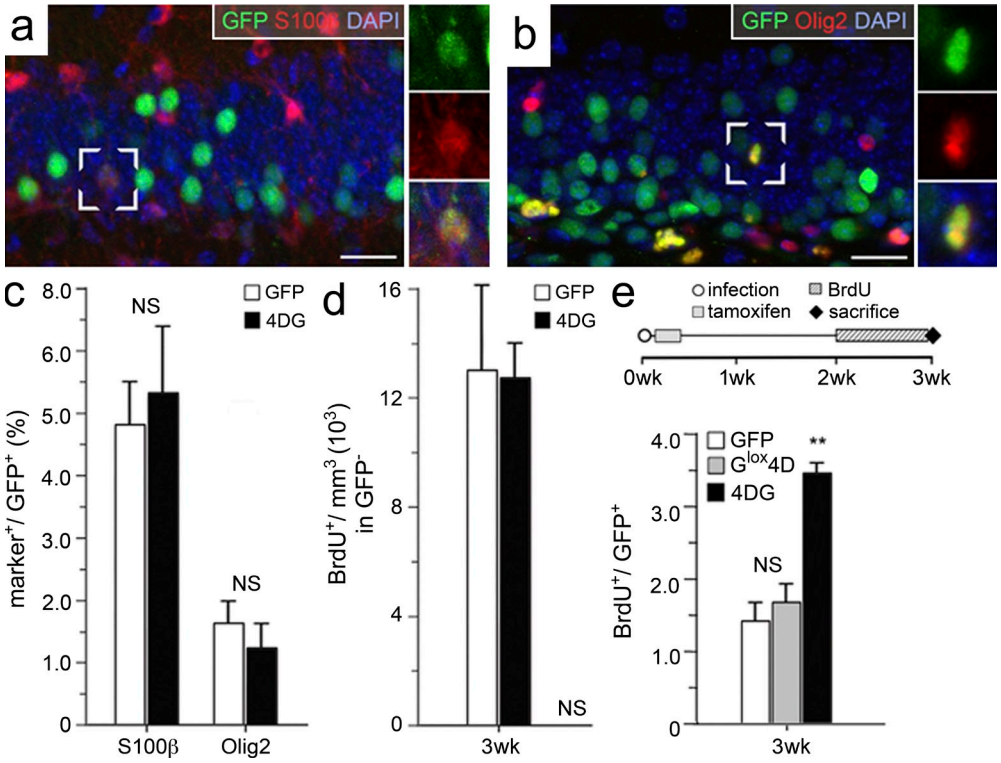

Figure 6. The effects of 4D are cell intrinsic. (a and b) Fluorescence pictures of the granular and subgranular zone 3 wk after infection with GFP viruses and immunohistochemistry for GFP, S100-β or Olig2 (a and b, respectively), and DAPI counterstaining. White frames indicate GFP^+ cells that have been scored as S100-β^+ (a) or $Olig2^+$ (b), whose individual channels are shown magnified in the right insets. Bars, 20 µm. (c) Proportions (percentages) of S100-β^+ and $Olig2^+$ cells among the GFP^+ population 3 wk after GFP or 4DG infection (all GFP^+ cells = 100%). (d) Absolute number of $BrdU^+$ GFP^- cells per cubic millimeter of granular plus subgranular zone 3 wk after GFP or 4DG infection. (e) Layout of the experiments and quantifications (gray bar) of $BrdU^+$ GFP^+ cells 3 wk after $G^{lox}4D$ infection in nestin-$CreER^{t2}$ mice with a 2-d tamoxifen administration starting 24 h after viral infection and BrdU administration performed during the 7 d preceding sacrifice. Data of wild-type mice infected with GFP or 4DG viruses (white and black bars, respectively) were taken from Fig. 2 d (3-wk time point) and added for better comparison. (c–e) Data are the mean of at least three hippocampi of different animals; error bars represent SD; **, $P < 0.001$; difference in c, d, and e (bottom, white and gray bars) is not significant.

In light of these opposing results, can findings in the developing brain be reconciled with our observations in the adult brain? We think that a likely explanation for the different effects of 4D overexpression on cell subpopulations of the developing as compared with the adult brain can be found in the opposite cell cycle kinetics observed in the two systems (Cameron and McKay, 2001; Hayes and Nowakowski, 2002; Seri et al., 2004; Calegari et al., 2005; Arai et al., 2011). In essence, it appears that 4D overexpression is simply more effective in changing the fate of either stem or progenitor cells with long cell cycles while having little or no effect on fast proliferating cells. This may be relevant for the many laboratories studying cell cycle regulation of somatic cells as it implies that 4D cannot shorten the cell cycle beyond its physiological minimal length, not even when it is overexpressed over long periods of time. In addition, in relation to the role of cell cycle length in stem cell differentiation (Lange and Calegari, 2010; Salomoni and Calegari, 2010), these data corroborate previous observations (Calegari et al., 2005; Lange et al., 2009), suggesting that a relative variation of the cell cycle is far more important for cell fate change than its absolute duration. In essence, having a long or short cell cycle in absolute terms is not necessarily crucial for the fate of a given cell, whereas a sudden variation in relative terms may lead to major effects. Clearly, more studies are needed to provide in-depth molecular insight into the mechanisms underlying changes in cell cycle/fate of somatic stem cells.

Another important observation of our study was that after termination of 4D overexpression neural stem and progenitor cells could resume physiological neurogenesis, which resulted in an increased neuronal production as a consequence of their previous increased expansion. This indicates that cell fate of NSCs can be temporarily manipulated and a normal balance between proliferation and neurogenesis restored, avoiding depletion of the stem cell pool or transformation of NSCs into cancer stem cells (model in Fig. 7). This latter point was particularly important because tumors are known to up-regulate cdks and/or cyclins, and thus, it was in principle possible that 4D overexpression might have tumorigenic effects.

Possible applications of an inducible expansion of adult NSCs

Our finding may provide a powerful new approach to better address the role of adult neurogenesis and the effects that increased expansion of NSCs may have in physiological or pathological conditions. We are confident that future functional studies will greatly benefit from a systematic characterization and optimization of the approach described here, which may include manipulating 4D expression, or its activity, by systems that are superior to viral infection with regard to reproducibility and efficiency, including the generation of transgenic lines or pharmacological means.

Moreover, even if a transitory overexpression of 4D allowed us to increase the generation of neurons among the pool of infected cells, it might be that under the current conditions, these additional neurons will not integrate in the neuronal circuitry as most newborn neurons are known to undergo physiological apoptosis (Kempermann et al., 2004; Imayoshi et al., 2008; Zhao et al., 2008). However, considering that stimuli can be used to increase survival and integration of newborn neurons, such as learning, enriched environment, or physical activity (Kempermann, 2008; Zhao et al., 2008), our finding may provide an important platform to investigate the role of adult neurogenesis in behavioral contexts proposed to involve neurogenesis. In fact, until now, approaches aimed at addressing this issue were based on blocking rather than increasing neurogenesis, which overall led to many inconclusive or controversial results (Deng et al., 2010).

In addition, it is known that neurogenesis decreases during life and that stimuli can be used to increase neurogenesis of aged mice to improve hippocampal activity (Kempermann et al., 2002; Drapeau and Nora Abrous, 2008). Thus, in the

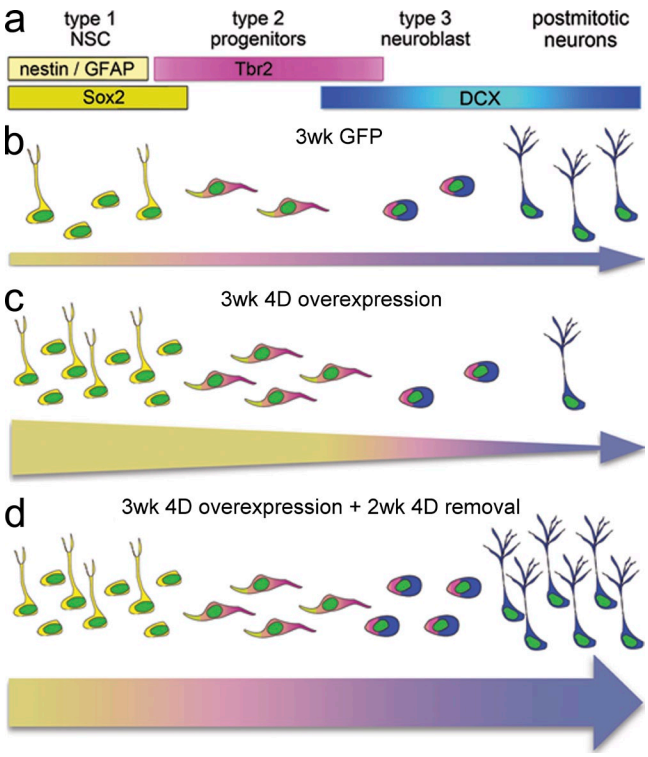

Figure 7. Proposed effect of 4D manipulation. (a–d) Markers used to assess the cell types of the adult hippocampus (a) with proportion of cells (b–d) approximately representing the values quantified in our study. Colored arrows underneath cells indicate the lineage from NSCs (yellow) to neurons (blue), with thickness representing the absolute number of cells progressing from one to the next cell population. (c) Note the increase in type 1 NSCs and type 2 progenitors upon 3-wk overexpression of the 4D complex with concomitant reduction in neurogenesis relative to control (b) as represented by a thickening of the left end of the arrow and thinning toward the right. (d) 3 wk of 4D overexpression followed by removal of the 4D cassette for an additional 2 wk induced a twofold increase in newborn neurons. In this case, proportions of other cell types were represented assuming a physiological balance between proliferation and differentiation as depicted by an arrow of the same proportion, but thicker, than in b.

future, it would be interesting to investigate whether 4D overexpression can be used to reproduce the increase in neurogenesis observed in stimulating environments and improve cognitive performance of senescent animals.

Finally, our approach may provide a new resource for using NSCs in models of neurodegenerative disease. In fact, NSCs are believed to be important for developing novel therapies for brain disorders (Goldman, 2005; Lindvall and Kokaia, 2006), and great efforts are invested worldwide to achieve this challenging goal. In this context, it is interesting to observe that certain brain injuries can trigger a transient shortening of G1 with a concomitant expansion of NSCs and inhibition of neurogenesis, as has been shown after stroke by the pioneering studies of Zhang et al. (2006, 2008). Thus, our manipulation of 4D seems to recapitulate, on a much bigger scale, a physiological response to injury, which may be important for brain recovery.

Cdk–cyclin complexes allow the manipulation of stem cell fate

It should be noticed that cdk–cyclin complexes (Lange et al., 2009), or even cyclins alone (Pilaz et al., 2009), were suggested to influence the proliferation versus differentiation not only of NSCs of the developing mouse embryo but also of other stem cell types, including embryonic (and perhaps also induced) pluripotent (Singh and Dalton, 2009) and hematopoietic (Orford and Scadden, 2008) stem cells (Lange and Calegari, 2010). Our work extends this general theme also to adult NSCs, strongly suggesting that manipulation of cdk–cyclin complexes can be used to control the expansion versus differentiation of any stem cell type. Although validation of this hypothesis still requires extensive studies in many tissues, our work may provide a useful new platform not only for studying neurogenesis but also for the whole field of stem cell research. In this context, it should be considered that many applications may not even require genetically modified organisms because cdk–cyclin-expressing viruses that also carry a $CreER^{t2}$ cassette could in principle be used. Finally, we believe that our study provides a proof of principle demonstrating that expansion versus differentiation of adult mammalian stem cells can be acutely manipulated and temporally controlled in vivo, which is of paramount importance for the use of somatic stem cells in therapy.

MATERIALS AND METHODS

Constructs and viral preparations. The cDNAs of GFP, RFP, cdk4, and cyclinD1 (Lange et al., 2009) were fused to T2A (de Felipe et al., 2006) or loxP sequences by PCR and cloned by conventional methods in HIV-1 or MLV transfer vectors. To avoid viral recombination, T2A sequences were chosen that contained as many base mutations as possible without change in amino acid sequence. Viruses were generated by polyethyleneimine transfection of 293T cells with the respective transfer vector together with the pCD/NL-BH (Mochizuki et al., 1998) and pczVSV-G (Pietschmann et al., 1999) vectors encoding for HIV-1 gag/pol structural proteins and vesicular stomatitis glycoprotein G, respectively (5 µg of each vector per 5×10^6 293T cells in a 10-cm dish). Constructs for the preparation of MLV were provided by F.H. Gage (Salk Institute for Biological Studies, La Jolla, CA) and used as previously described (Lie et al., 2005). After 24 h, cells were induced with 10 mM *n*-butyric acid (Sigma-Aldrich), and 1 d later, supernatants were collected and centrifuged for 1.5 h at 120,000 *g*, and the viral particles were resuspended in 10 µl PBS per dish, usually yielding a titer of 10^8–10^9/ml as assessed by titration on HeLa cells.

Biochemistry. Lysates of HeLa cells infected with GFP, RFP, 4DG, or 4DR viruses were loaded on NuPAGE 4–12% Bis-Tris gels and transferred to nitrocellulose. Membranes were blocked with 5% milk in TBS with 1% Tween for 1 h at room temperature and primary antibodies (Table S1) incubated overnight at 4°C. After washing, membranes were incubated with horseradish peroxidase–coupled secondary antibodies for 2 h at room temperature. Luminescence (ECL Plus system; GE Healthcare) was developed, and non-saturated radiograms were analyzed with ImageJ 1.33 software (National Institutes of Health). Stripping (0.1 M glycine, pH 2.0, for 15 min twice) was used for α-tubulin detection for internal normalization.

Stereotaxic injection and drug administration. 1.5-µl viral suspensions were stereotaxically injected into 6–10-wk-old, isoflurane-anaesthetized, C57/Bl6 or nestin-$CreER^{t2}$ (Imayoshi et al., 2008) female mice, the latter provided by R. Kageyama (Institute for Virus Research, Kyoto University, Kyoto, Japan), using an injector (Nanoliter 2000; World Precision Instruments) and a stereotaxic frame (model 900; Kopf Instruments) at ±1.6 mm mediolateral, −1.9 anterior–posterior, and −1.9 mm dorsoventral from bregma. Brains were collected 1 wk or more later, eventually after BrdU and/or tamoxifen administration (1 mg/mouse or 5 mg/mouse dissolved in 100 µl or 50 µl PBS or corn oil, respectively) by repetitive injections at 12-h intervals for 7 d or 2 d, respectively (except for the determination of label retaining cells, for which BrdU injections were repeated at 24-h intervals). Animal experiments were approved by local authorities (24D-9168.11-1/2008-16 and 2007–2).

Immunohistochemistry. Mice were perfused with 4% PFA (except for DCX immunohistochemistry because we observed better specificity in non-perfused brains), and brains were postfixed in 4% PFA overnight at 4°C. Coronal, 40-µm thick vibratome sections through the hippocampus were serially grouped, collecting one section every six, and eventually stored at −20°C in cryoprotectant solution (50% phosphate buffer 1 M, 25% ethylene glycol, and 25% glycerol). Single groups were used to perform immunohistochemistry for GFP, BrdU, and/or at least one of the markers described (Table S1). In brief, sections were blocked in 10% donkey serum and permeabilized in 0.3% Triton X-100 in PBS for 1.5 h, and antibodies were diluted in 3% donkey serum (Jackson ImmunoResearch Laboratories, Inc.) and 0.3% Triton X-100 in PBS. Primary and secondary antibodies (see Table S1 for a detailed list and conditions) were incubated for 36 h and 12 h, respectively, at 4°C. DAPI was used to stain nuclei. Because Tbr2 labeling required boiling, and in our conditions boiling destroys GFP-epitope recognition, sections that required Tbr2 GFP double staining were labeled for GFP, pictures were acquired, and then sections were boiled to perform Tbr2 immunolabeling. In these cases, DAPI counterstaining was used as a reference to digitally merge the resulting pictures. In all experiments, GFP immunohistochemistry was performed to enhance endogenous fluorescence. Fluorescence composite pictures of the hippocampus were acquired using an automated microscope (ApoTome; Carl Zeiss), cell numbers and areas in each group of sections were assessed (with several samples being counted blind by two people; Fig. S2) on electronic files, and pictures were assembled and analyzed using Photoshop CS4 (Adobe) or ImageJ 1.33.

Statistical analyses. Analyses were performed on $n \geq 3$, with n being defined as an entire hippocampus of one mouse. Percentages obtained from different hippocampi were used to calculate mean, SD, and significance by two-tailed Student's t test analysis, assuming unequal variance or analysis of variance when appropriate.

Online supplemental material. Fig. S1 depicts the criteria used to identify DCX^+ type 3 neuroblasts from DCX^+ newborn neurons in the adult mouse hippocampus. Fig. S2 summarizes the number of GFP^+-infected cells

counted in each experiment and those positive for any other marker used in this study. Table S1 indicates the antibodies and conditions used in this study. Online supplemental material is available at http://www.jem.org/cgi/content/full/jem.20102167/DC1.

We are very grateful to Dr. Fred H. Gage for providing the MLV vectors, Dr. Ryoichiro Kageyama for the nestin-CreER^{t2} line, and Christiane Rubbert and the staff of the animal facility of the Max Planck Institute of Molecular Cell Biology and Genetics for technical support. We also thank Drs. Gerd Kempermann, Magdalena Götz, Dietmar Chichung Lie, Karen Echeverri, Ravi Jagasia, and Shahryar Khattak for helpful discussion and advice.

B. Artegiani was supported by a fellowship of the Dresden International Graduate School for Biomedicine and Bioengineering program, Dresden. F. Calegari was supported by the Center for Regenerative Therapies, the Medical Faculty of the Dresden University of Technology, and the German Research Foundation Collaborative Research Center SFB655 (subproject A20).

B. Artegiani and F. Calegari have submitted a patent application concerning the data described in this manuscript (EP10160288.6). The authors have no remaining conflicts of interest.

Author contributions: B. Artegiani and F. Calegari planned the experiments 30:70, performed the experiments 100:0, analyzed data 50:50, and prepared the manuscript 10:90. D. Lindemann generated the transfer viral vector p6NST90.

Submitted: 12 October 2010
Accepted: 15 March 2011

REFERENCES

Arai, Y., J.N. Pulvers, C. Haffner, B. Schilling, I. Nüsslein, F. Calegari, and W.B. Huttner. 2011. Neural stem and progenitor cells shorten S-phase on commitment to neuron production. *Nat Commun*. 2:154. doi:10.1038/ncomms1155

Calegari, F., W. Haubensak, C. Haffner, and W.B. Huttner. 2005. Selective lengthening of the cell cycle in the neurogenic subpopulation of neural progenitor cells during mouse brain development. *J. Neurosci*. 25:6533–6538. doi:10.1523/JNEUROSCI.0778-05.2005

Cameron, H.A., and R.D. McKay. 2001. Adult neurogenesis produces a large pool of new granule cells in the dentate gyrus. *J. Comp. Neurol*. 435:406–417. doi:10.1002/cne.1040

de Felipe, P., G.A. Luke, L.E. Hughes, D. Gani, C. Halpin, and M.D. Ryan. 2006. E unum pluribus: multiple proteins from a self-processing polyprotein. *Trends Biotechnol*. 24:68–75. doi:10.1016/j.tibtech.2005.12.006

Deng, W., J.B. Aimone, and F.H. Gage. 2010. New neurons and new memories: how does adult hippocampal neurogenesis affect learning and memory? *Nat. Rev. Neurosci*. 11:339–350. doi:10.1038/nrn2822

Drapeau, E., and D. Nora Abrous. 2008. Stem cell review series: role of neurogenesis in age-related memory disorders. *Aging Cell*. 7:569–589. doi:10.1111/j.1474-9726.2008.00369.x

Goldman, S. 2005. Stem and progenitor cell-based therapy of the human central nervous system. *Nat. Biotechnol*. 23:862–871. doi:10.1038/nbt1119

Hayes, N.L., and R.S. Nowakowski. 2002. Dynamics of cell proliferation in the adult dentate gyrus of two inbred strains of mice. *Brain Res. Dev. Brain Res.* 134:77–85. doi:10.1016/S0165-3806(01)00324-8

Hevner, R.F., R.D. Hodge, R.A. Daza, and C. Englund. 2006. Transcription factors in glutamatergic neurogenesis: conserved programs in neocortex, cerebellum, and adult hippocampus. *Neurosci. Res.* 55:223–233. doi:10.1016/j.neures.2006.03.004

Hodge, R.D., T.D. Kowalczyk, S.A. Wolf, J.M. Encinas, C. Rippey, G. Enikolopov, G. Kempermann, and R.F. Hevner. 2008. Intermediate progenitors in adult hippocampal neurogenesis: Tbr2 expression and coordinate regulation of neuronal output. *J. Neurosci*. 28:3707–3717. doi:10.1523/JNEUROSCI.4280-07.2008

Imayoshi, I., M. Sakamoto, T. Ohtsuka, K. Takao, T. Miyakawa, M. Yamaguchi, K. Mori, T. Ikeda, S. Itohara, and R. Kageyama. 2008. Roles of continuous neurogenesis in the structural and functional integrity of the adult forebrain. *Nat. Neurosci*. 11:1153–1161. doi:10.1038/nn.2185

Kempermann, G. 2008. The neurogenic reserve hypothesis: what is adult hippocampal neurogenesis good for? *Trends Neurosci*. 31:163–169. doi:10.1016/j.tins.2008.01.002

Kempermann, G., D. Gast, and F.H. Gage. 2002. Neuroplasticity in old age: sustained fivefold induction of hippocampal neurogenesis by long-term environmental enrichment. *Ann. Neurol*. 52:135–143. doi:10.1002/ana.10262

Kempermann, G., S. Jessberger, B. Steiner, and G. Kronenberg. 2004. Milestones of neuronal development in the adult hippocampus. *Trends Neurosci*. 27:447–452. doi:10.1016/j.tins.2004.05.013

Kriegstein, A., and A. Alvarez-Buylla. 2009. The glial nature of embryonic and adult neural stem cells. *Annu. Rev. Neurosci*. 32:149–184. doi:10.1146/annurev.neuro.051508.135600

Lange, C., and F. Calegari. 2010. Cdks and cyclins link G1 length and differentiation of embryonic, neural and hematopoietic stem cells. *Cell Cycle*. 9:1893–1900. doi:10.4161/cc.9.10.11598

Lange, C., W.B. Huttner, and F. Calegari. 2009. Cdk4/cyclinD1 overexpression in neural stem cells shortens G1, delays neurogenesis, and promotes the generation and expansion of basal progenitors. *Cell Stem Cell*. 5:320–331. doi:10.1016/j.stem.2009.05.026

Lie, D.C., S.A. Colamarino, H.J. Song, L. Désiré, H. Mira, A. Consiglio, E.S. Lein, S. Jessberger, H. Lansford, A.R. Dearie, and F.H. Gage. 2005. Wnt signalling regulates adult hippocampal neurogenesis. *Nature*. 437:1370–1375. doi:10.1038/nature04108

Lindvall, O., and Z. Kokaia. 2006. Stem cells for the treatment of neurological disorders. *Nature*. 441:1094–1096. doi:10.1038/nature04960

Lugert, S., O. Basak, P. Knuckles, U. Haussler, K. Fabel, M. Götz, C.A. Haas, G. Kempermann, V. Taylor, and C. Giachino. 2010. Quiescent and active hippocampal neural stem cells with distinct morphologies respond selectively to physiological and pathological stimuli and aging. *Cell Stem Cell*. 6:445–456. doi:10.1016/j.stem.2010.03.017

Mochizuki, H., J.P. Schwartz, K. Tanaka, R.O. Brady, and J. Reiser. 1998. High-titer human immunodeficiency virus type 1-based vector systems for gene delivery into nondividing cells. *J. Virol*. 72:8873–8883.

Orford, K.W., and D.T. Scadden. 2008. Deconstructing stem cell self-renewal: genetic insights into cell-cycle regulation. *Nat. Rev. Genet*. 9:115–128. doi:10.1038/nrg2269

Pietschmann, T., M. Heinkelein, M. Heldmann, H. Zentgraf, A. Rethwilm, and D. Lindemann. 1999. Foamy virus capsids require the cognate envelope protein for particle export. *J. Virol*. 73:2613–2621.

Pilaz, L.J., D. Patti, G. Marcy, E. Ollier, S. Pfister, R.J. Douglas, M. Betizeau, E. Gautier, V. Cortay, N. Doerflinger, et al. 2009. Forced G1-phase reduction alters mode of division, neuron number, and laminar phenotype in the cerebral cortex. *Proc. Natl. Acad. Sci. USA*. 106:21924–21929. doi:10.1073/pnas.0909894106

Salomoni, P., and F. Calegari. 2010. Cell cycle control of mammalian neural stem cells: putting a speed limit on G1. *Trends Cell Biol*. 20:233–243. doi:10.1016/j.tcb.2010.01.006

Seri, B., J.M. García-Verdugo, L. Collado-Morente, B.S. McEwen, and A. Alvarez-Buylla. 2004. Cell types, lineage, and architecture of the germinal zone in the adult dentate gyrus. *J. Comp. Neurol*. 478:359–378. doi:10.1002/cne.20288

Shen, Q., Y. Wang, E. Kokovay, G. Lin, S.M. Chuang, S.K. Goderie, B. Roysam, and S. Temple. 2008. Adult SVZ stem cells lie in a vascular niche: a quantitative analysis of niche cell-cell interactions. *Cell Stem Cell*. 3:289–300. doi:10.1016/j.stem.2008.07.026

Singh, A.M., and S. Dalton. 2009. The cell cycle and Myc intersect with mechanisms that regulate pluripotency and reprogramming. *Cell Stem Cell*. 5:141–149. doi:10.1016/j.stem.2009.07.003

Suh, H., A. Consiglio, J. Ray, T. Sawai, K.A. D'Amour, and F.H. Gage. 2007. In vivo fate analysis reveals the multipotent and self-renewal capacities of Sox2+ neural stem cells in the adult hippocampus. *Cell Stem Cell*. 1:515–528. doi:10.1016/j.stem.2007.09.002

Tang, W., I. Ehrlich, S.B. Wolff, A.M. Michalski, S. Wölfl, M.T. Hasan, A. Lüthi, and R. Sprengel. 2009. Faithful expression of multiple proteins via 2A-peptide self-processing: a versatile and reliable method for manipulating brain circuits. *J. Neurosci*. 29:8621–8629. doi:10.1523/JNEUROSCI.0359-09.2009

Tavazoie, M., L. Van der Veken, V. Silva-Vargas, M. Louissaint, L. Colonna, B. Zaidi, J.M. Garcia-Verdugo, and F. Doetsch. 2008. A specialized

vascular niche for adult neural stem cells. *Cell Stem Cell*. 3:279–288. doi:10.1016/j.stem.2008.07.025

van Praag, H., A.F. Schinder, B.R. Christie, N. Toni, T.D. Palmer, and F.H. Gage. 2002. Functional neurogenesis in the adult hippocampus. *Nature*. 415:1030–1034. doi:10.1038/4151030a

Zarkowska, T., and S. Mittnacht. 1997. Differential phosphorylation of the retinoblastoma protein by G1/S cyclin-dependent kinases. *J. Biol. Chem*. 272:12738–12746. doi:10.1074/jbc.272.19.12738

Zhang, R.L., Z.G. Zhang, M. Lu, Y. Wang, J.J. Yang, and M. Chopp. 2006. Reduction of the cell cycle length by decreasing G1 phase and cell cycle reentry expand neuronal progenitor cells in the subventricular zone of adult rat after stroke. *J. Cereb. Blood Flow Metab.* 26:857–863. doi:10.1038/sj.jcbfm.9600237

Zhang, R.L., Z.G. Zhang, C. Roberts, Y. LeTourneau, M. Lu, L. Zhang, Y. Wang, and M. Chopp. 2008. Lengthening the G(1) phase of neural progenitor cells is concurrent with an increase of symmetric neuron generating division after stroke. *J. Cereb. Blood Flow Metab.* 28:602–611. doi:10.1038/sj.jcbfm.9600556

Zhao, C., W. Deng, and F.H. Gage. 2008. Mechanisms and functional implications of adult neurogenesis. *Cell*. 132:645–660. doi:10.1016/j.cell.2008.01.033